Laminar flame velocities and fundamental properties for two methane based mixtures: G27 and G222

Kodjo Coudoro[1, 2], Nabiha Chaumeix[2], Bentaïb Ahmed[1], C-E Paillard[2]
[1]IRSN, France; [2] ICARE Orleans

1 Introduction

The 18th century marked the beginning of the industrial era. Since then, mankind's consumption of energy has been increasing as well as the need of energy. With the developing industries and their growing number, come various risks. Amongst these, the accidental ignition of a combustible gaseous mixture in an industrial environment is of great concern. The ignition sources in such accidental situations are mainly a spark or the contact of the gaseous mixture with a hot surface leading therefore to a laminar deflagration with relatively slow burning velocities, under certain conditions, these flames can accelerate and undergo transition to detonation generating overpressures high enough to cause severe material damage. Predicting and understanding the process of flame acceleration then became crucial for the prevention of such industrial hazards. Most of flame acceleration studies focused on hydrogen/air systems and led to a better knowledge of the conditions for hydrogen/air mixtures' acceleration which led to the definition of a criterion to discriminate between slow and fast flames: "sigma criterion". Others systems such as natural gas systems have been less studied. In order to extend this criterion to natural gas it is mandatory to gain the fundamental knowledge necessary for such an analysis: laminar flame properties of the targeted mixtures. Hence, we first need to construct a strong database based both on experimental and modeling data to derive those properties.

The aim of the present work is to determine the fundamental properties of natural gas – air by studying two methane based mixtures (G27 and G222) and evaluate their potential for flame acceleration in a highly instrumented acceleration tube (acceleration study is under process). The laminar flame velocities and Markstein lengths were determined experimentally by studying the expanding spherical flames in a combustion bomb using high speed imaging coupled to a schlieren optical setup. The experimental laminar flames speed data were used in order to validate a detailed kinetic mechanism for natural gas combustion based on published mechanisms using COSILAB - 1D freely propagating flame. The transport properties as well as the flame temperature, the maximum theoretical pressure and the expansion ratio were estimated using CHEMKIN II equilibrium calculations.

2 Experimental facility and methodology

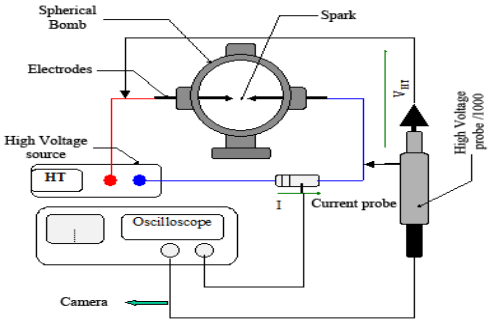

Figure 1: Ignition Layout.

Correspondence to: kodjo.coudoro@cnrs-orleans.fr

The experimental setup used in this work is composed of a stainless steel spherical combustion chamber (476 mm diameter and 56L). The chamber is equipped with two quartz windows (97 mm diameter) in order to provide an optical access during flame propagation. The ignition layout is presented on fig.1 and consists in a high voltage source coupled to two electrodes inside the chamber used to form a spark in the middle of the combustion chamber to initiate the combustion. The visualization of the propagating flame is obtained by shadowgraphy method. A high speed camera records the images of the evolution of the flame front which allow us to evaluate the flame radius as a function of time.

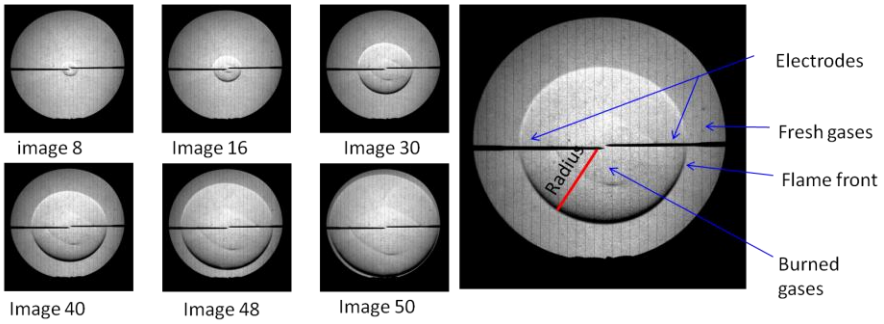

Figure 2: Temporal evolution of the flame front (E.R=1.25, P=1bar, T=303K, G27-Air)

Fig.2 shows the images recorded by the camera and the evolution of the flame radius as a function of time.

The mixtures were prepared directly in the chamber using the partial pressure method. The gases used during this work are G27 (82% CH_4 and 18%N_2) which we assume to be the least reactive representative of natural gas due to its high content in nitrogen and G222 (77% CH_4 and 23%H_2) which we assume to be the most reactive since it contains more than 20% of hydrogen. Both gases are provided by Air Liquide France

Methodology

The methodology used to derive the laminar flame velocity on the basis of the data acquired with the high speed camera was largely exposed by Lamoureux et al. [1] and Halter et al. [2]. The data provided by camera recordings (Fig. 2) are processed to derive the spatial velocity of the flame front.

In the case of a spherically propagating flame, it was shown by Eschenbach and Agnew [3] that the laminar flame velocity S_L is expressed (when the pressure is constant) as the ratio between the spatial flame velocity V_S and the expansion factor of the burnt gases σ: $S_L = \frac{V_s}{\sigma}$.

Furthermore, as the spherically propagating flame is submitted to curvature and strain effects that modify the flame surface, the effect of stretch is to be taken into account, during the evaluation of the laminar flame velocity. The stretched flame velocity V_s and the unstretched flame velocities V_s^0 are linked by two coefficients known as the Markstein length L and κ the stretch rate of the spherically expanding flame.

The following relation was proposed by Clavin (1985) [4].

$$V_S = V_S^0 - L \cdot \kappa$$

The fundamental flame velocity is also submitted to stretch effects:

$$S_L = S_L^0 - L' \cdot \kappa$$

Where L' represents the Markstein length divided by the expansion factor and S_L^0 the unstretched fundamental flame velocity.

During flame propagation, we are able to record the pressure rise in the combustion chamber using a Kistler pressure sensor mounted inside the chamber. Figure 3 and Figure 4 show the pressure rise in the chamber as a function of the time as well as the visualization window. By monitoring the pressure

during the combustion, it is shown that the pressure remains constant during flame visualization justifying the use of the constant pressure assumption at the early stages of the flame propagation. Furthermore, as mentioned in section 2, the visualization of the flame is only possible for diameters lower than 97mm. When the flame reaches this diameter, the burnt gases volume is approximately 0.8% of the total volume of the bomb and cannot result in any pressure increase as shown on figure 4.

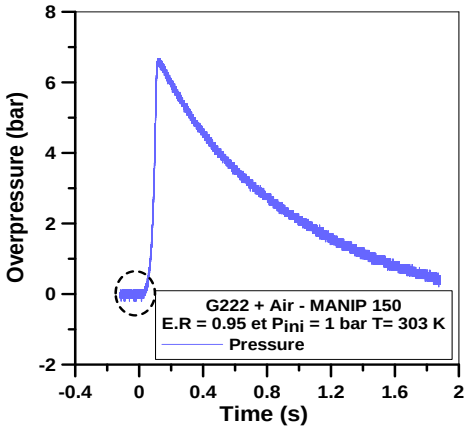

Figure 3: Pressure rise in the chamber for a G222/Air mixture, E.R 0.95, P=1bar and T=303K

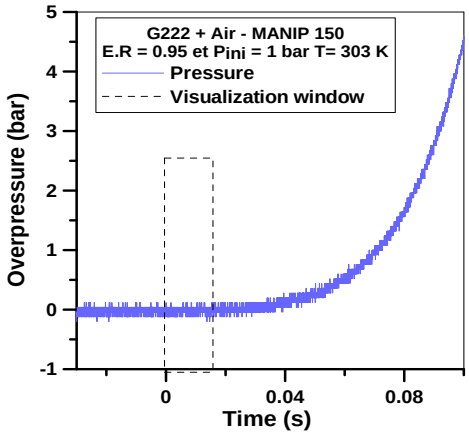

Figure 4: Zoom on visualization window for a G222/Air mixture, E.R 0.95, P=1bar and T=303K

This methodology was validated by Lamoureux et al.[1] over H_2/air mixtures and compared to several data available in the literature (Liu et al. [5], Koroll et al. [6], Dowdy et al. [7], Egolfopoulos et al. [8], Raman [9] and Aung et al. [10]) on H_2/air laminar flame velocity as it is shown on figure 5. The velocities measured by Lamoureux et al. show an excellent agreement with the data of the literature. The difference with the data measured by Liu et al. and Koroll et al. is due to the fact that early studies didn't take the effect of stretch on the flame into account leading to higher values of the laminar flame speed than those reported by the recent studies.

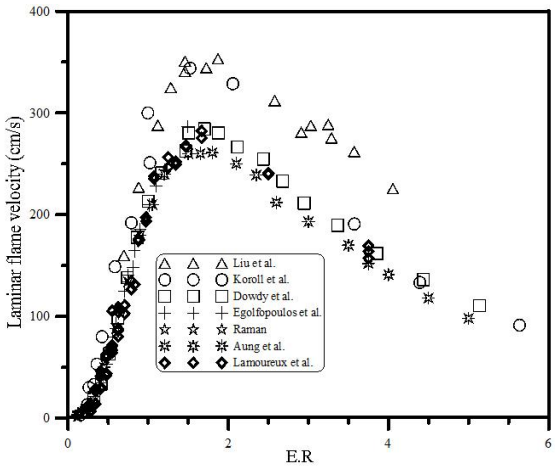

Figure 5 : Laminar flame velocity for H_2/air mixtures and comparison with the literature

3 Experimental results and modeling

3.1 Laminar flame speeds and Markstein lengths for G222 at 1 bar and 303K

On Figure 6 is plotted the evolution of the laminar flame speed against the equivalence ratio As there is no data in the literature on G222/Air, we compare our experimental data to those on methane/air mixtures available in the literature (Gu et al. [11], Hassan et al. [12], Bradley et al. [13], Coppens et al. [14], Tahtouh et al. [15]). The presence of hydrogen in our mixture results in higher values of the laminar flame speed of G222 when compared to those of methane/air mixture. This was mentioned by Halter et al. [2] and Tahtouh et al. [16]. The plots exhibit a bell shaped evolution, increasing from the lean side to the rich and reaching a maximum value for an equivalence ratio of 1.1. The corresponding flame speed for G222 air/mixtures is 47.2 cm/s.

On Figure 7, we show the evolution of the Markstein length against the equivalence ratio for an ambient temperature and pressure. The increasing equivalence ratio results in increasing the Markstein length. Also the Markstein length remains positive sign of the flame stability. It is to be noticed that, as mentioned by Lamoureux et al.[1], that the uncertainties in the derivation of the Markstein length may be important due to the method of derivation.

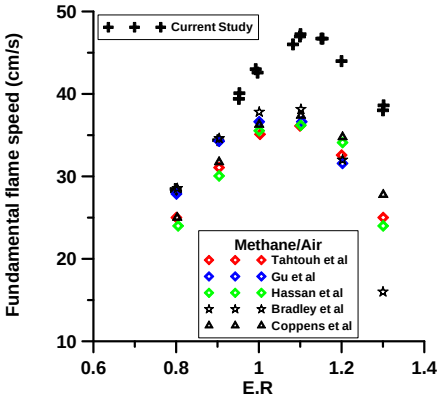

Figure 6 : Fundamental flame speed against equivalence ratio for G222/Air (P=100kPa, T=303K)

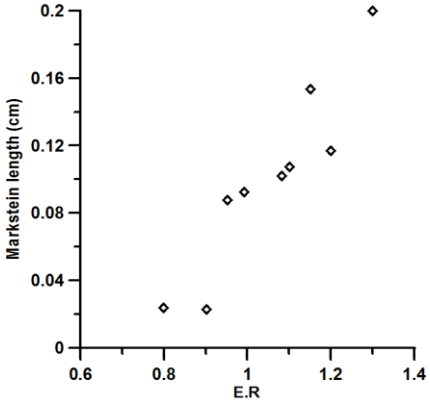

Figure 7 : Markstein length against equivalence ratio for G222/Air (P=100kPa, T=303K)

3.2 Laminar flame speeds and Markstein lengths for G27 at 1 bar and 303K

On Figure 8 is represented the evolution of the laminar flame speed for G27/Air mixtures as a function of the equivalence ratio. As there is a lack of experimental data in the literature on G27, we compare our experimental data to those published on methane/air mixtures (Gu et al. [11], Hassan et al. [12], Bradley et al. [13], Coppens et al. [14], Tahtouh et al. [15]) and on Natural gas/air mixtures (Liao et al. [17]). As expected, we notice that the curve for G27/air mixtures is lower than those for methane/air mixtures and natural gas/air mixtures. This is due to the lower oxidation rate resulting from the dilution in nitrogen in the case of G27. The plot of the laminar flame speed as a function of the equivalence ratio describes a characteristic bell shaped curve. The velocity increases as the equivalence ratio increases up to a maximum value of 35.27 cm/s corresponding to an equivalence ratio of 1.05 and then decreases whilst the equivalence ratio gets higher than 1.05

On Figure 9, we plotted the Markstein lengths against the equivalence ratio and compared them to those published on methane/air mixtures by Bradley et al. [13], Gu et al. [11] and Tahtouh et al. [15]. We can notice that the measured Markstein lengths our experiments are in the same order of magnitude with the data from the literature. As mentioned for G222/air mixtures, we notice the increase of the Markstein length alongside the equivalence ratio and that the Markstein lengths remain positive indicating the flame stability.

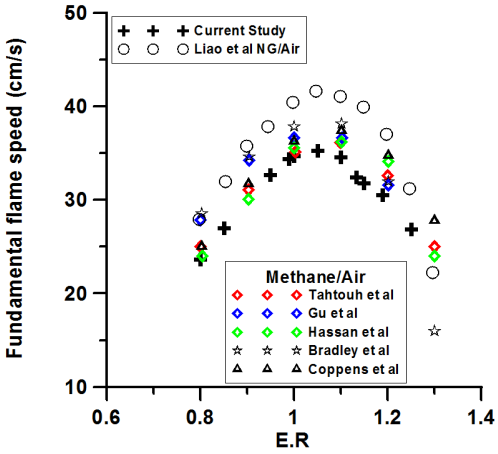

Figure 8 : Fundamental flame speed against equivalence ratio for G27/Air (P=100kPa, T=303K)

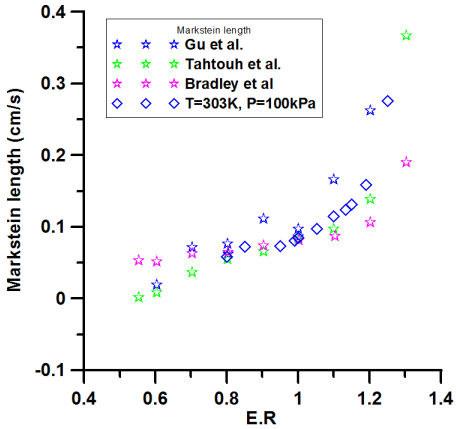

Figure 9 : Markstein length against equivalence ratio for G27/Air (P=100kPa, T=303K)

3.3 Kinetic modeling of G222/air and G27/air mixtures

The measured laminar flame velocities have been modeled using three kinetic models from the literature and Softpredict's software Cosilab®. The kinetic mechanisms tested were:

1. The GRI 3.0 developed at the Gas research institute with 53 species and 325 reactions
2. The Galway mechanism for methane/propane oxidation at high pressure with 118 species and 663 reactions
3. The USC mech II, developed at the university of south California consisting in 111 species and 784 reactions

Figure 10 and figure 11 display the comparison between the modeling with the three mentioned kinetic models and, respectively, G27/air and G222/air mixtures. In the case of G27/air mixtures, it shows that the GRI and Curran mech overestimate the flame velocity over the whole equivalence ratio range while the USC mech overestimates S_L^0 on the lean side and then underestimates it on the rich side. All three mechanisms predict the equivalence ratio (1.05) corresponding to the highest value of S_L^0. Concerning G222/air mixtures, all three mechanisms overestimate S_L^0 on the lean side and underestimate on the rich side with the USC mech giving significantly lower values than the other mechanisms. Here the three mechanisms predict the maximum velocity for an equivalence ratio of 1.05 while the experiments display the maximum velocity for the equivalence ratio of 1.1

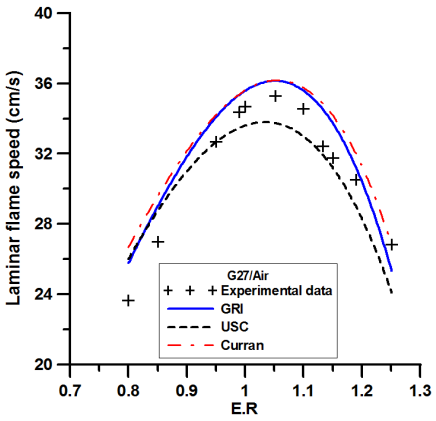

Figure 10 : Experimental data versus modeling G27/Air

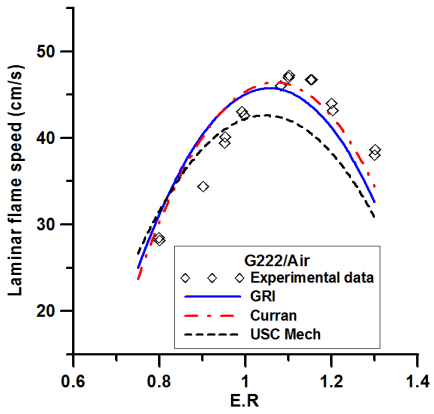

Figure 11 : Experimental data versus modeling G222/Air

Conclusion

Experiments were conducted using the spherical bomb method to measure laminar flame velocities and Markstein lengths for two methane based mixtures G222 and G27. Data will be provided for several temperatures and pressure. Using the chosen detailed chemical kinetic mechanism aforementioned, the activation energies will be derived from the evolution of laminar flame velocities as a function of the flame temperature (COSILAB - 1D freely propagating flame). Also, a kinetic investigation will be made to understand and explain the differences between the experimental and modeling data for all three mechanisms. Experiments will also be conducted in an acceleration tube in order to evaluate an acceleration criterion for both mixtures.

1. Lamoureux, N., N. Djebaïli-Chaumeix, and C.E. Paillard, *Laminar flame velocity determination for H2-air-He-CO2 mixtures using the spherical bomb method.* Experimental Thermal and Fluid Science, 2003. **27**(4): p. 385-393.
2. Halter, F., et al., *Characterization of the effects of pressure and hydrogen concentration on laminar burning velocities of methane-hydrogen-air mixtures.* Proceedings of the Combustion Institute, 2005. **30**(1): p. 201-208.
3. Eschenbach, R.C. and J.T. Agnew, *Use of the constant-volume bomb technique for measuring burning velocity.* Combustion and Flame, 1958. **2**(3): p. 273-285.
4. Clavin, P., *Dynamic behavior of premixed flame fronts in laminar and turbulent flows.* Progress in Energy and Combustion Science, 1985. **11**(1): p. 1-59.
5. Liu, D.D.S. and R. MacFarlane, *Laminar burning velocities of hydrogen-air and hydrogen-air---steam flames.* Combustion and Flame, 1983. **49**(1-3): p. 59-71.
6. Koroll, G.W., R.K. Kumar, and E.M. Bowles, *Burning velocities of hydrogen-air mixtures.* Combustion and Flame, 1993. **94**(3): p. 330-340.
7. Dowdy, D.R., et al., in *Twenty-Third Symposium (International) on Combustion*. 1993, The Combustion Institute: Pittsburgh. p. 325–332.
8. Egolfopoulos, F.N. and C.K. Law, in *Twenty-Third Symposium (International) on Combustion*. 1990, The Combustion Institute: Pittsburgh. p. 333–340.
9. Raman, K.S. 1998, Explosion Dynamics Laboratory.
10. Aung, K.T., M.I. Hassan, and G.M. Faeth, *Flame stretch interactions of laminar premixed hydrogen/air flames at normal temperature and pressure.* Combustion and Flame, 1997. **109**(1-2): p. 1-24.
11. Gu, X.J., et al., *Laminar burning velocity and Markstein lengths of methane-air mixtures.* Combustion and Flame, 2000. **121**(1-2): p. 41-58.
12. Hassan, M.I., K.T. Aung, and G.M. Faeth, *Measured and predicted properties of laminar premixed methane/air flames at various pressures.* Combustion and Flame, 1998. **115**(4): p. 539-550.
13. Bradley, D., P.H. Gaskell, and X.J. Gu, *Burning velocities, markstein lengths, and flame quenching for spherical methane-air flames: A computational study.* Combustion and Flame, 1996. **104**(1-2): p. 176-198.
14. Coppens, F.H.V., J. De Ruyck, and A.A. Konnov, *Effects of hydrogen enrichment on adiabatic burning velocity and NO formation in methane + air flames.* Experimental Thermal and Fluid Science, 2007. **31**(5): p. 437-444.
15. Tahtouh, T., F. Halter, and C. Mounaïm-Rousselle, *Measurement of laminar burning speeds and Markstein lengths using a novel methodology.* Combustion and Flame, 2009. **156**(9): p. 1735-1743.
16. Tahtouh, T., et al., *Effects of hydrogen addition and nitrogen dilution on the laminar flame characteristics of premixed methane-air flames.* International Journal of Hydrogen Energy, 2009. **34**(19): p. 8329-8338.
17. Liao, S.Y., D.M. Jiang, and Q. Cheng, *Determination of laminar burning velocities for natural gas.* Fuel, 2004. **83**(9): p. 1247-1250.